Jestr

Journal of Engineering Science and Technology Review 9 (4) (2016) 37-47

Research Article

JOURNAL OF
Engineering Science and Technology Review

www.jestr.org

Time-of-arrival and Direction-of-arrival Estimation Techniques for IR-UWB Signals

D. Santhosh Kumar* and V.V. Mani

Department of Electronics and Communication Engineering, National Institute of Technology, Warangal, Telangana, India-506004

Received 22 January 2016; Accepted 23 September 2016

Abstract

This paper deals with how a ultra wideband signal (UWB) can be used to estimate time of arrival (TOA) and direction of arrival (DOA). The paper has also elucidated a comparative study of the performance of the four algorithms used for TOA estimation, namely multiple signal classification (MUSIC), deconvolution, maximum likelihood (ML) estimation and two stage estimation under the multipath non-line-of-sight (NLOS) channel conditions given in IEEE 802.15.3a model. MUSIC has given the best result in terms of accuracy. Coherent signal subspace method (CSM) of DOA estimation works well for a wideband signal by condensing the wide subspace into a narrow subspace using focusing matrices. The frequency to which the wide subspace is focused is called the focusing frequency and is calculated by minimizing a certain subspace fitting error. The above algorithm has been chosen because it involves MUSIC, which has this innate ability to separate multipath components, thereby making it the best choice for multipath channels.

Keywords: TOA, DOA, focusing matrix, weighted signal subspace, MUSIC

1. Introduction

The interest in the field of ultra wideband (UWB) signals has renewed given the modern day radio has exhausted all the possible frequency ranges and UWB unlike the current carrier based modulation dates back to the early concept of pulsed radio thereby making the system less complex [1]. Its attributes like high frequency and large bandwidth enhances signal propagation through walls and high temporal resolution respectively. Additionally a large bandwidth improves reliability as the signal contains different frequency components which increases the possibility that at least some of them will go through and around obstacles. UWB has an additional advantage to offer, if we look at it from the interference mitigation point of view. The spreading of the pulses over a large bandwidth and the subsequent lowering of the power spectral density (PSD) reduces interference to other systems. It is precisely these above mentioned properties that make UWB a desirable choice for indoor positioning applications. The primary operation that is needed for such an application is ranging. Several such UWB transceivers with the help of estimates of the direction and distance of a UWB transmitting nodes cumulatively locate its exact coordinates. Therefore time of arrival (TOA) and direction of arrival (DOA) estimation plays a crucial role in a generalized positioning system. Till now work has been done on TOA estimation for single path and multipath line-of-sight (LOS) conditions. When looked at from a practical point of view the channels are usually non-line-of-sight (NLOS) in nature. The comparative study of the algorithms is done from varied dimensions ranging from estimation accuracy, complexity of computations involved, robustness against multipath components. A brief overview of the ranging techniques in multipath environment is given in [2]. As per the requirement of the application the desired algorithm can be chosen. So far work has been done in the field of indoor positioning of UWB nodes using the TOA and DOA techniques [3] under LOS multipath channel conditions. Joint TOA and DOA estimation has been proposed in [4].TOA estimation can be done in both time and frequency domains and a comparison between them is stated in [5]. The work was extended in [6] where in the author has substantiated the effect of the number of receiving elements on estimation accuracy, with the help of ranging

* E-mail address: skumar@nitw.ac.in

estimation error graphs. In [7] methods based on minimum variance are proposed for wireless positioning systems. A joint TOA and DOA estimation compliant with IEEE 802.15.4a is given in [8]. DOA plays a crucial role in beamforming and its estimation methodology under ideal channel single path conditions is proposed in [9]- [10]. A coherent signal subspace method (CSM) [11] that does not require preliminary DOA estimates uses the eigen vector matrix of the received signal to compute optimal focusing matrices. Another technique for focusing matrix computation [12] involves minimizing the signal Eigen vector's focusing error and DOA estimation bias error. The following paper is organized as follows. Section 2 mathematically explains the transmitted time hopped-pulse position modulated (THPPM) UWB signal. In addition to that it also explains the nature of channels that constitute the IEEE 802.15.3a channel model (CM) based on Saleh-Valenzuela (S-V) model. Section 3 elaborates on the mathematical and conceptual part of the four algorithms used. Section 4 will take you through the coherent subspace method that has been adopted to estimate the DOA. A few real time applications explained with figures are given in section 5. The results in the form of TOA estimation error versus signal to noise ration (SNR) graph for CM2, CM3, CM4 channels and the DOA estimation graphs are given in section 6. It also covers the inferences derived from simulation results presenting a comparative analysis of the algorithms. The paper is concluded in section 7.

2. System and Channel Model

Some of the properties of UWB and the channel models are presented in the following sub sections.

2.1 Properties of UWB Pulse

- **Fine time resolution:** Since UWB pulses are extremely short they can be filtered or ignored [13]. They can readily be distinguished from unwanted multipath reflections. This leads to the characteristic of multipath immunity.
- **Large bandwidth:** Provides extremely high data rates [14] leading to high spectral capacity.
- **Reduced cost:** There is no need for translating the UWB to further high frequencies therefore we do not require expensive and large components such as modulators, demodulators and intermediate frequency (IF) stages. The only cost incurred is in the frequency hopping set up.
- **Low PSD:** This property enables low probability of detection [15] which is of particular interest for military applications like covert communications and radar.

Impulse radio ultra wideband (IR-UWB) pulse transmitted is of sub nanosecond duration. The UWB monocycle [16] is the second order derivative of a Gaussian pulse.

$$p(t) = \left[1 - 4\pi\left(\frac{t}{\tau_m}\right)^2\right]\exp\left[-2\pi\left(\frac{t}{\tau_m}\right)^2\right] \quad (1)$$

where τ_m is the impulse width parameter, approximately 0.4 times the pulse width. We consider a TH-PPM version of the UWB monocycle [17] is given by

$$s_q(t) = \sum_j P\left(t - jT_f - c_j^q T_c - \delta d^q\right) \quad (2)$$

Where j is the frame number, q is the user number, T_f is the duration of a frame, T_c is the chip duration, δ is the duration for which the pulse is to be shifted if the bit transmitted is 1, d^q is the symbol of the q^{th} user and c_j^q is the sequence or code value corresponding to the j^{th} frame and q^{th} user. In Fig.1, the TH-PPM signal corresponding to one user is presented. As per the code the monopulses are spread across the frames. The code assigned to a single user in the Fig.1 is [0 2 0]. So the pulse in the first frame is in the 0^{th} chip, the pulse in the 2^{nd} frame is in the 2^{nd} chip and so on

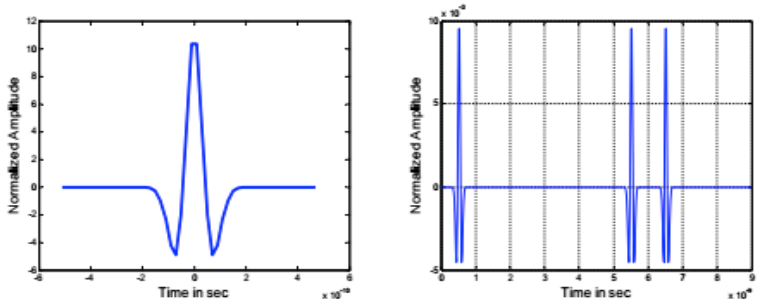

Fig. 1. UWB pulse and its PPM version

2.2 IEEE 802.15.3a Channel Model

The IEEE 802.15.3a channel model is a stochastic channel model based on the S-V model [18] where multipath components arrive in clusters. The S-V model representation of the channel is given by

$$h(t) = X\sum_{k=0}^{K-1}\sum_{l=0}^{L-1}\alpha_{k,l}\exp\left(j\theta_{k,l}\right)\delta\left(t-T_l-\tau_{k,l}\right) \quad (3)$$

Where T_l is the arrival time of the cluster, $\tau_{k,l}$ is the time delay of the k^{th} ray in the l^{th} cluster, $\theta_{k,l}$ is the uniformly distributed phase in the range of $[0,2\pi]$, $\alpha_{k,l}$ is the multipath gain coefficients of the k^{th} ray in the l^{th} cluster and X describes the log-normal shadow fading of all the multipath.

The arrival time T_0 of the first cluster is zero for LOS models and exponentially distributed with intensity Λ for NLOS models. Four different types of channels have been modeled under IEEE 802.15.3a. The characteristics of these channels are given in Table.I.

Table 1. IEEE 802.15.3a Channel Model

Parameter	CM 1	CM 2	CM 3	CM 4	Unit
Tx-Rx separation	0-4	0-4	4-10		m
LOS/NLOS	LOS	NLOS	NLOS	NLOS	
Mean excess delay	5	9.9	15.9	30.1	ns
RMS delay	5	8	15	25	ns

Paths in CM1 and CM2 tend to concentrate in two or three clusters with a smaller delay, whereas in CM3 and CM4 paths tend to spread over more clusters and have bigger delay. This is due to their different cluster arrival rates. The gains of paths in CM3 and CM4 decay faster due to their longer path. As is evident the paths in CM4 are closely spaced as compared to CM2, CM3 and CM1.

The TH-PPM UWB pulse given in (2) convolved with the channel impulse response in (3) gives the following equation.

$$x(t) = \sum_{m=0}^{M-1}\sum_{q=1}^{Q}h_m s_q\left(t-\tau_m\right)+n(t) \quad (4)$$

Where h_m is the gain coefficient of the m^{th} path and M is the number of paths in the multipath channel. Representation of (4) in the frequency domain is given as follows.

$$X(\omega) = \sum_{m=0}^{M-1}\sum_{q=1}^{Q}h_m S_q(\omega)e^{-j\omega\tau_m}+N(\omega) \quad (5)$$

Where $X(\omega)$, $S_q(\omega)$ and $N(\omega)$ denote the Fourier transform of the received signal, transmitted signal and noise, respectively. Sampling and rearranging (4) into a matrix notation the received signal vector at the q antenna element is given by,

$$\boldsymbol{X}_q = \sum_{m=0}^{M-1}h_m\boldsymbol{S}_q\boldsymbol{e}_{\tau_{mq}}+\boldsymbol{N}_q \quad (6)$$

Where the elements of vector $\boldsymbol{X}_q$, $\boldsymbol{X}_q(\omega_n)$ are the DFT components of $X(\omega)$ with $(\omega_n)=(\omega_0 n)$ for $n=0,1,....,N-1$ and $\omega_0=\frac{2\pi}{N}$, $\boldsymbol{S}_q$ is a diagonal matrix whose elements are the DFT coefficients of the transmitted signal and the noise samples are arranged in vector $\boldsymbol{N}_q$. The elements of the delay signature vector include the dependency with the angle of arrival in τ_{mq}

$$\boldsymbol{e}_{\tau_{mq}} = \left[1 \quad e^{-j\omega_0\tau_{mq}} \quad e^{-2j\omega_0\tau_{mq}} \quad ..... \quad e^{-(N-1)j\omega_0\tau_{mq}}\right] \quad (7)$$

Where τ_{mq} denotes the delay associated with the m^{th} path and the q^{th} source.

3. Algorithms for TOA Estimation

Moreover the received and the original TH-PPM signals are normalized before applying the respective algorithm.

3.1 ML Estimation

It is a correlation based estimator. If Gaussian noise is added then ML criterion is equivalent to the minimum mean squared error (MMSE) criterion [19].

$$\tau_{est} = \arg\max_{\tau}\left(\boldsymbol{Y}^T(\tau)\boldsymbol{R}^{-1}(\tau)\boldsymbol{Y}(\tau)\right) \quad (8)$$

Where $\boldsymbol{Y}(\tau)$is the correlation between the received signal (4) and the shifted versions of the original transmitted signal $\boldsymbol{S}(\tau)$and $\boldsymbol{R}$is the autocorrelation matrix of the transmitted signal $\boldsymbol{S}(\tau)$given in (2), $R(\tau) = E\left[S(\tau)^T S(\tau)\right]$. The above equation can be rewritten as

$$\tau_{est} = \arg\max_{\tau}\left(E\left(S^T(\tau)x\right)^T E\left(S^T(\tau)S(\tau)\right)^{-1} E\left(S^T(\tau)x\right)\right) \quad (9)$$

The correlation and autocorrelation is calculated for the signal matrices shifted at different values of τ. The value of τ are those time instants at which the amplitude of the convolved signal x is within the range of 10dB from the peak.

- Pros: ML based methods separate the paths serially one by one. This approach mitigates the multipath effect in a ranging system. In addition, no prior information is needed for the implementation of ML-based methods.
- Cons: It is not effective for highly closely spaced multipath components. It is least sensitive to noise.

3.2 Two Stage Estimation

This algorithm is implemented in the frequency domain and is done in two stages. In the first stage of estimation we make a rough estimate of the time instant of the first arriving path. In the second stage we fine tune rough estimate to the closest approximation possible.

- **Coarse estimation:** This step basically identifies the beginning of the symbol in the received signal. We identify the time duration by which the first symbol has been shifted with respect to the original TH-PPM UWB signal [20]. In the presence of noise and a distorted channel there is a fair chance that the convolved signal might not contain the first monopulse of the TH-PPM signal. Therefore the first step involved is calculating the frame number to which the first pulse in the received signal belongs. This involves the principle of energy detector. The energy of the received signal which also includes noise, is calculated and the location of the peaks of the energy denotes the position of the pulse in the received signal. The relative distance between the N_f peaks can be represented as

$$\Delta_\alpha = \left[(\alpha_2 - \alpha_1) \ \ldots\ldots \ (\alpha_j - \alpha_{j-1}) \ \ldots\ldots \ (\alpha N_f - \alpha N_{f-1})\right] \quad (10)$$

Where α_n denotes the position of the n^{th} peak. The time hopping code sequence can be described as $c = \left[c_1 \ \ c_2 \ \ c_3 \ \ldots\ldots \ c_{N_f}\right]$. We define a cyclic matrix whose row elements denote the relative spacing between two monocycles in terms of chip delays.

$$\rho_c(n) = N_c - c_n - c_{n-1} \quad (11)$$

Where N_c is number of chips per frame, N_f is number of frames and c_n denotes the code corresponding to the n^{th} frame.

$$\{\Delta\} = \begin{Bmatrix} \rho_c(1) & \rho_c(2) & \rho_c(3) & \ldots & \rho_c(N_f-1) & \rho_c(N_f) \\ \rho_c(2) & \rho_c(3) & \rho_c(4) & \ldots & \rho_c(N_f) & \rho_c(1) \\ \ldots & & & & & \\ \rho_c(N_f) & \rho_c(1) & \ldots & \ldots & \rho_c(N_f-2) & \rho_c(N_f-1) \end{Bmatrix} \quad (12)$$

The algorithm then compares $\Delta_\alpha(10)$ with each of the rows of the circular matrix $\Delta(12)$. The row number corresponding to the row that is closest to Δ_α gives us the frame number to which the first symbol belongs. The relative shift given by τ_{coarse} between the first arriving monopulse and its corresponding location in the original transmitted symbol is calculated.

$$\tau_{coarse} = \left| T_{chip} c_v - T_s P_k \right| \quad (13)$$

Where T_{chip} is the chip duration, v is the frame number to which the first pulse belongs to, P_k represents the location of the first peak, T_s is the sampling time duration and c_v is the time hopping code corresponding to the v^{th} frame

- **Fine estimation:** Estimation of correlation matrix corresponding to the k^{th} symbol is done using the frequency domain samples of the received signal given in (6).

$$\boldsymbol{R}_k = \frac{1}{N_f} \boldsymbol{X}_k \boldsymbol{X}_k^H \quad (14)$$

Where matrix

$$X_k = \left[X_1^k \quad X_2^k \quad .... \quad X_{N_f}^k \right] \quad (15)$$

Where each column constitutes the elements of the frame wise DFT of the received signal. The power delay profile is calculated as follows for different possible values of τ.

$$P_k(\tau) = \boldsymbol{e}_\tau^H \boldsymbol{R}_k \boldsymbol{e}_\tau \quad (16)$$

Where $\boldsymbol{e}_\tau$ is the delay signature vector given in (7). It is of dimension $[1XN]$, where N is the length of the DFT. Power threshold value denoted by P_{th} is the noise power calculated in the coarse estimation stage

$$\tau_{fine} = \min_{\tau} \arg P_k(\tau) > P_{th} \quad (17)$$

The final estimated value of time of arrival is given by

$$\tau_{est} = \tau_{fine} + \tau_{coarse} \quad (18)$$

3.3 MUSIC Algorithm

The subspace based algorithms involve the decomposition of the space spanned by the observation vector (i.e., the vector formed by the received signal samples) into several subspaces, usually a noise subspace and a signal subspace. These algorithms use the orthogonality property between noise and signal subspaces to estimate channel parameters. The steering vector for one value of τ is given by

$$Steer(\tau) = \left[1 \quad e^{-j2\pi \frac{1}{N} f_s \tau} \quad e^{-j2\pi \frac{2}{N} f_s \tau} \quad .... \quad e^{-j2\pi \frac{N-1}{N} f_s \tau} \right] \quad (19)$$

Where N is the length of the DFT sequence. The vector is of dimension $[1XN]$ and the value of τ is varied for over a wide range of values. Using the vector given in (6) we get the correlation matrix $\boldsymbol{P}$

$$\boldsymbol{P} = \boldsymbol{X}_q \boldsymbol{X}_q^T \quad (20)$$

Where $\boldsymbol{P}$ turns out to be a $[NXN]$ matrix. The correlation matrix hence is eigen decomposed resulting in N eigen values and an eigen vector matrix of dimension $[NXN]$. The eigen vector subspace is divided into signal subspace which is of dimension $[NXQ]$ and a noise subspace given by $\boldsymbol{U}_n$ of dimension $[NX(N-Q)]$. It follows the simple explanation that the noise subspace is orthogonal to the signal subspace. To calculate the pseudospectrum for a range of values of τ the vector Steer is multiplied with the noise subspace vector $\boldsymbol{U}_n$

$$H(\tau) = \frac{1}{Steer(\tau) U_n U_n^T Steer(\tau)^T} \quad (21)$$

The value of τ for which H encounters the first peak is the estimated time of arrival.

- **Pros:** This algorithm gives the best results in terms of its ability to separate multipath components, as it utilizes the principle of orthogonality between noise and signal subspace. Since it separates noise and signal subspaces this method is preferred in areas where noise interference is high.
- **Cons:** The complexity of the algorithm poses serious limitation on its use in applications which cannot support complex hardware.

3.4 Deconvolution Method

Deconvolution methods are essentially inverse filters. The received signal at a sensor element is translated to the frequency domain.

$$X(f) = S(f)H(f) + N(f) \quad (22)$$

As the name suggests deconvolution is the dual of the convolution operation in the time domain. The RHS and LHS of (22) is divided by the frequency domain version of the original transmitted UWB signal (4).

$$\boldsymbol{S}^{-1}\boldsymbol{X} = \boldsymbol{H} + \boldsymbol{W} \quad (23)$$

This will give us the frequency response of the channel. In the vector form it can be written as $\boldsymbol{Y} = \boldsymbol{H} + \boldsymbol{W}$, where $\boldsymbol{Y} = \boldsymbol{S}^{-1}\boldsymbol{X}$ and $\boldsymbol{W} = \boldsymbol{S}^{-1}\boldsymbol{N}$

- **Pros:** Deconvolution produces better results than correlation methods in terms of its ability to resolve between closely spaced multipaths. Though the resolution is nothing compared to the resolution that MUSIC offers. The simplicity of this algorithm adds to its advantages.
- **Cons:** One of the adverse effects that deconvolution poses is due to inverse filtering. This method is unfavorable in the presence of noise as it leads to noise enhancement. Due to the involvement of computation of inverse matrix, the requirement for memory is high.

4. DOA Estimation using Coherent Signal Subspace Processing

The importance of estimation of DOA lies in beamforming, indoor positioning and radar sensing applications. One of the methods that was adopted for DOA estimation [21] used multiple frequency invariant beamformers. Such methods though efficient need a beamformer structure whereas the coherent signal subspace method (CSM) just requires an antenna array. Signal subspace spans the location vectors of the array for fixed DOAs. We condense the wide subspace into a narrow subspace using focusing matrices. DOA estimation system using an antenna array and five-port circuit is described in [6] for detecting arrival angles in the azimuth plane of signals pitched by the antenna array. Another technique for DOA estimation using weighted signal subspace has been proposed in [12]. One of the common approaches adopted for wideband signal processing is incoherent signal subspace method (ISSM). It divides the wide frequency band into several narrow bands and each one of them is subjected to narrow band signal-subspace method. The results from each narrow band is then averaged. For cases where sources are correlated this method fails. In order to overcome the drawbacks associated with ISSM the widespace is focused into a narrow band space. Based on this [12] has proposed a method of calculating optimal focusing matrices. The frequency at which the wide sub space needs to be focused is chosen at random. The above proposed technique works for a channel that gets instantaneously mixed with the incoming signal. Direction finding for UWB sources without the prior knowledge of initial angle of arrival estimates [11] was done using auto focusing. But this method fails in the presence of channel conditions similar to the ones modelled in IEEE 802.15.3a. The problem statement considered here involves the presence of NLOS multipath channels modelled under IEEE 802.15.3a group and the mixing is convolutive in nature. Therefore a prior rough estimate of DOA is needed. The focusing matrix is calculated and an optimal focusing frequency is obtained by iterative minimization of an error. Once the signal space of the wideband signal is focused to the optimal narrow band space what follows is simple application of MUSIC algorithm. The entire procedure can be divided in the following steps:

- Calculation of the location vectors for the entire range of frequencies observed
- Calculation of focusing matrix
- Calculation of optimum focusing frequency
- The newly obtained subspace is subjected to MUSIC algorithm and DOA is estimated

4.1 Location Vector

A location vector gives us the information about the prior rough DOA estimates of the wideband signals at different elements of the antenna array.

$$A(\omega_k, \phi) = \left[a(\omega_k, \phi_1) \quad .... \quad a(\omega_k, \phi_Q) \right] \quad (24)$$

$$a(\omega_k, \phi_q) = \left[1 \quad e^{-j\omega_k \frac{d_1}{c}\sin(\phi_q)} \quad .... \quad e^{-j\omega_k \frac{d_L}{c}\sin(\phi_q)} \right] \quad (25)$$

$$\phi = \begin{bmatrix} \phi_1 & .... & \phi_Q \end{bmatrix} \quad (26)$$

Where Q is the number of sources and L is the number of antenna array elements.

4.2 Calculation of Focusing Matrix

The focusing matrix [12] satisfies the following property (27) and it has a dimension of $[LXL]$.

$$T^H(\omega_k)T(\omega_k) = I \quad (27)$$

$$T(\omega_k) = V(\omega_k)U(\omega_k)^H \quad (28)$$

$$A(\omega_k)A(\omega_0)^H = U(\omega_k)\sum V(\omega_k)^H \quad (29)$$

Where V and U are the left and right singular vectors and $A(\omega_0)$ is the location vector calculated at an optimum frequency.

4.3 Calculation of Optimum Focusing Frequency

The fundamental principle behind the calculation of focusing frequency is to minimize the subspace fitting error using least squares minimization. An iterative procedure is adopted where the initial optimum frequency is assumed to be f_{mid}. The matrix (33) denoting the subspace fitting error is observed iteratively for frequencies being incremented at the rate of $\Delta_f = (1/N)f_s$ and the frequency that results in the minimum value gives the optimal focusing frequency. Focusing frequency selection plays a very crucial role in the calculation of the focusing subspace, [22] gives an optimized algorithm for the same

$$f_{\min} = (1/N)f_s \quad (30)$$

$$f_{\max} = f_s \quad (31)$$

$$f_{mid} = \frac{f_{\min} + f_{\max}}{2} \quad (32)$$

The work in [23] explains mathematically to minimize a tight bound to the error. In the following equations we have denoted $A(\omega_k)$ as A_{ω_k} and $A(\omega_0)$ as A_0. Subspace fitting error can be mathematically represented as

$$\sum_{k=0}^{N-1} \left\| A_0 - T_{\omega_k} A_{\omega_k} \right\|^2 \quad (33)$$

The optimum frequency is given as

$$\omega_{opt} = \arg\min_{\omega_k} \left\| A_0 - T_{\omega_k} A_{\omega_k} \right\|^2 \quad (34)$$

We follow certain Lemmas to expand the Frobenious form and calculate the optimum focusing frequency.

- **Lemma 1:** The Frobenious matrix (33) is expanded as

$$\sum_{k=0}^{N-1} \left[\|A_0\|^2 + \|A_{\omega_k}\|^2 - 2\,\mathrm{Re}\,tr\left(A_0 A_{\omega_k} T_{\omega_k}\right) \right] \quad (35)$$

$$= 2J_{pq} - 2\sum_{k=0}^{N-1}\sum_{i=0}^{q} \sigma_i \left(A_0 A_{\omega_k}^H\right) \quad (36)$$

J_{pq} is constant so the subject of variation is

$$2\sum_{k=0}^{N-1}\sum_{i=0}^{q} \sigma_i \left(A_0 A_{\omega_k}^H\right) \quad (37)$$

which can be expressed as

$$\sigma_i(B), i = 1,2,.....q \quad (38)$$

Where $B = A_0 A_{\omega_k}$ and q is the number of singular values of the vector B. Singular values of vector B is given in eqn (38). Therefore the minimization problem changes to the maximization of

$$\max_{\omega_k} \sum_{k=0}^{N-1}\sum_{i=0}^{q} \sigma_i \left(A_0 A_{\omega_k}^H\right) \quad (39)$$

- **Lemma 2:** It states that

$$\sum_{k=0}^{N-1}\sum_{i=0}^{q} \sigma_i \left(A_0 A_{\omega_k}^H\right) \le \sum_{k=0}^{N-1}\sum_{i=0}^{q} \sigma_i (A_0)\sigma_i \left(A_{\omega_k}\right)^H \quad (40)$$

The value of ω_k for which the R.H.S of the above equation obtains maximum value is said to be the optimum focusing frequency.

4.4 MUSIC Algorithm

The correlation matrix given in (20) is multiplied by the focusing matrix and this weighted correlation matrix is subjected to MUSIC algorithm.

$$G = \sum_{k=0}^{N-1} T(\omega_k) P_x(\omega_k) T(\omega_k)^H \quad (41)$$

The MUSIC algorithm eigen decomposes the weighted correlation matrix given in (41) giving L eigen values and an eigen vector matrix of dimension $[LXL]$. The eigen vector subspace is divided into signal subspace which is of dimension $[LXQ]$ and a Noise subspace given by U_n of dimension $[LX(L-Q)]$. It follows the simple explanation that the Noise subspace is orthogonal to the signal subspace. The steering vector is given by the following equation.

$$Steer(\phi) = \begin{bmatrix} 1 & e^{-j\omega_{opt}\frac{d}{c}\sin\phi} & .... & e^{-j\omega_{opt}(L-1)\frac{d}{c}\sin\phi} \end{bmatrix} \quad (42)$$

Where d is the inter element spacing and c is the speed of light. The pseudospectrum calculated at different values of ϕ is given by

$$H(\phi) = \frac{1}{Steer(\phi)\boldsymbol{U}_n\boldsymbol{U}_n^T Steer(\phi)^T} \quad (43)$$

The location of the first n peaks of the pseudospectrum H, represent the angle of arrival from n sources.

5. Applications

TOA and DOA estimation is needed for localization and ranging, which in turn forms the crux of the following applications. The challenges faced and applications are mentioned in [13].

5.1 UWB in Radar Sensing

In conditions of poor visibility a UWB sensing system can help two cars to maintain a safe distance, in order to avoid rear end collisions. Each car needs to be equipped with a UWB transmitter and receiver. Using the TOA and DOA estimation algorithms a car can accurately estimate the distance between itself and the cars trailing behind it as shown in Fig 2.

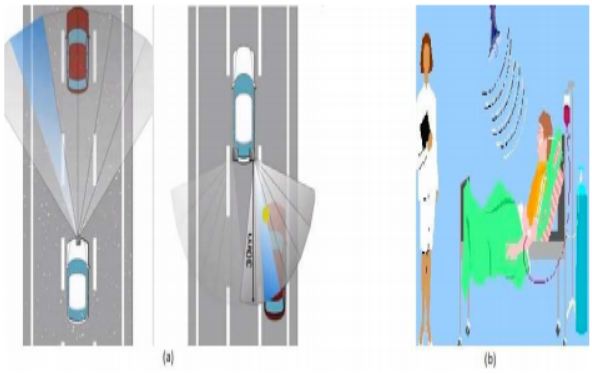

Fig. 2. UWB applications (a) radar sensing (b)patient motion monitoring

5.2 Indoor Localization

UWB provides for an economical alternative to localization [24] in areas where GPS is ineffective. Indoor localization in factories for the tracking of inventory in warehouse or cargo ships can be done using UWB nodes. A joint TOA and DOA estimation is required to identify the exact position.

5.3 Medical Applications

UWB owing to its low PSD ensures minimum radiation and interference, therefore it can be put to use in hospitals for patient motion monitoring. The UWB transmitter emitting a continuous impulse radio signal needs to be fixed on the ceiling as shown on in Fig 2. The IR-UWB signals get reflected when they meet human body. When the patient moves, the reflected signal will change its DOA. This change in DOA is interpreted at the receiver denoting the movement of the patient. This information could then be fed back instantaneously to the doctors or nurses.

6. Results

6.1 TOA Estimation and Comparison

The results have been consolidated in the form of performance graphs which depict the variation in the root mean square (RMS) error of the estimated TOA with increasing SNR. The performance of all the four algorithms can be explained in a nutshell by analyzing the results from various dimensions. For TOA estimation more the number of Monte Carlo simulations better will be the accuracy. But if the number of simulations are increased the processing time of the module increases rendering it inefficient.

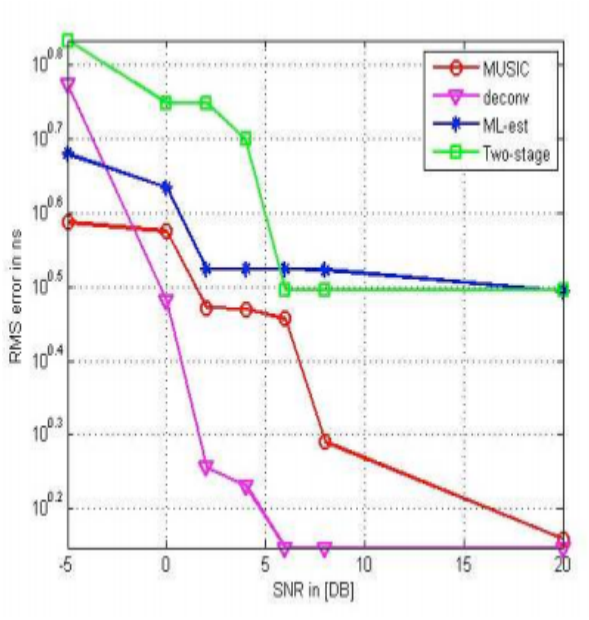

Fig. 3. Performance graph for CM2 channel

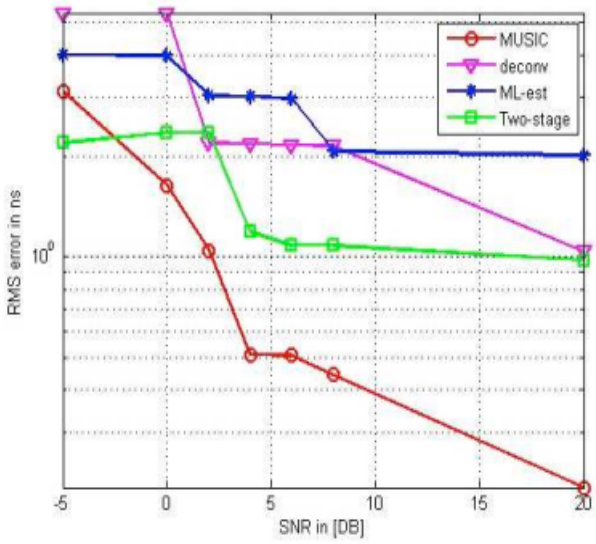

Fig. 4. Performance graph for CM3 channel

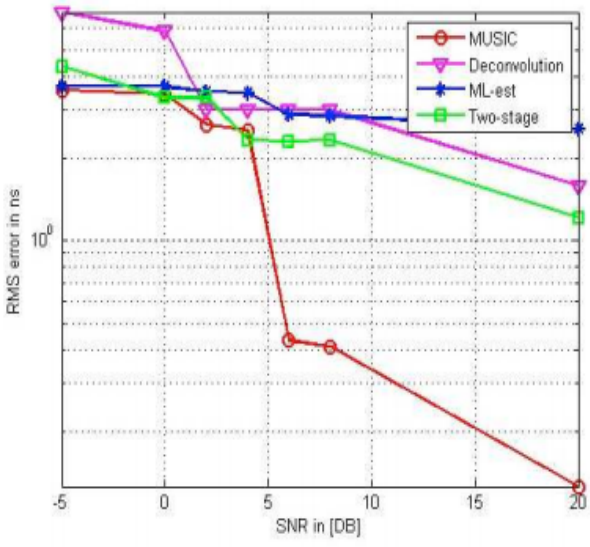

Fig. 5. Performance graph for CM4 channel

The comparison of the four algorithms is done on the following grounds

- **Ability to distinguish between multipaths:** The number of multipaths increases as we move from CM2-CM4. From the results Fig.3-5 one can infer that MUSIC has the ability to clearly distinguish between closely spaced multipaths since it works by separating the signal subspace and noise subspace. In Fig.5 the MUSIC has shown a steep decrease in the TOA estimation while other algorithms have not exhibited the same behavior. The number of sources is to be known prior in order to be able to separate the space into signal and noise.
- **Sensitivity to SNR:** ML estimation is least sensitive to variation in SNR as it considers only those paths that lie within the range of 10 dB from the peak. As can be seen from Fig 3-5 for all the three channel conditions the TOA estimation error has shown minimal drop for increasing SNR. MUSIC shows a steep change in its accuracy as we increase the SNR.
- **Complexity of the algorithm:** In terms of complexity deconvolution offers the best solution. But it is not a very favorable option under conditions of high noise interference. MUSIC has the maximum complexity due to the involvement of tedious computations in it.
- **Accuracy and complexity tradeoff:** ML estimation and two stage estimation offer the best solution in terms of a justified compromise between complexity and accuracy. But with the advent of fast processors that can handle complex calculations and high sampling rates MUSIC seems to be the best choice.

6.2 DOA Estimation using Coherent Subspace

Two sources and three antenna elements with an inter element spacing of $\lambda/2$ were considered. Table 2 shows the results. White Gaussian noise was added to the channel so as to maintain a SNR of 10dB. The entire procedure for DOA estimation was done in frequency domain owing to the subnano second duration of the Gaussian monopulse. The coherent subspace method for DOA estimation focuses a wideband subspace to a narrowband space by scaling the signal with the focusing matrix. The focusing matrix is obtained by the constrained least squares minimization. The narrowband subspace chosen should be such

that it minimizes the subspace fitting error. The received signal is then weighted with the power spectral density of the TH-PPM signal. The pseudospectrum of this resultant weighted signal in the narrowband subspace gives us the estimated DOA and it can be seen from Fig 6-8.

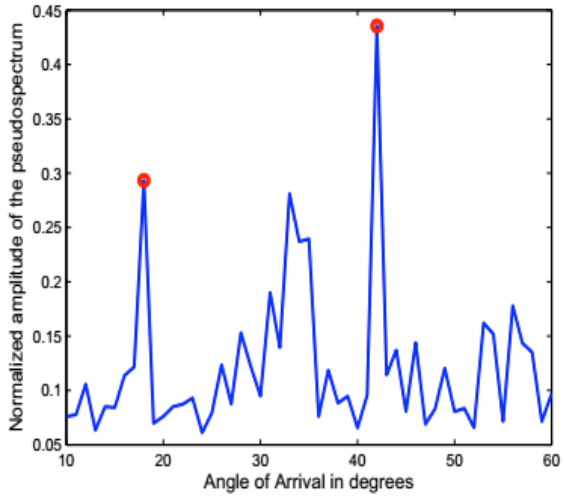

Fig. 6. Pseudospectrum vs Angle in degree for CM2 channel

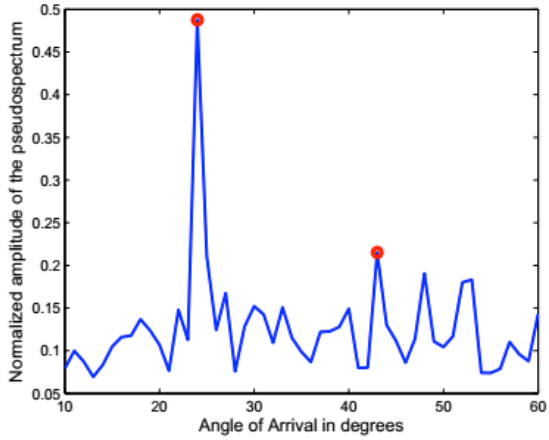

Fig. 7. Pseudospectrum vs Angle in degree for CM3 channel

Table 2. Estimated DOA values for different channel models

Channel type	Estimated DOA from source 1	Error in estimation for source 1	Estimated DOA from source 1	Error in estimation for source 1
CM 2	18^0	2^0	42^0	2^0
CM 3	24^0	4^0	42^0	2^0
CM 4	19^0	1^0	47^0	7^0

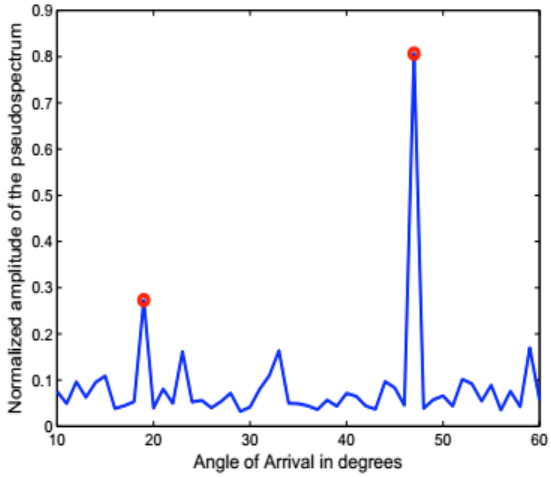

Fig. 8. Pseudospectrum vs Angle in degree for CM4 channel

7. Conclusions

The major contribution of this paper is TOA and DOA estimation of UWB signals. TOA of UWB signals is estimated using different algorithms in IEEE 802.15.3a channel environment. The comparison of the algorithms is done in various dimensions like their ability to distinguish between multipaths, sensitivity to SNR, complexity and Accuracy. Two stage estimation offer the best solution in terms of accuracy and complexity tradeoff. DOA estimation is done using coherent signal subspace method (CSM). Simulation results for DOA estimation show that as we go from CM2 to CM4 the error in estimation increases. This is due to the fact that the paths are closely spaced in CM4 and CM3 as compared to CM2 thereby making the resolvability tedious. Moreover the paths experience a faster decay as we go from CM2-CM4, resulting in a weaker received signal. Some of the practical impulse radio-ultra wideband (IR-UWB) applications is also discussed.

References

1. R. Aiello and A. Batra, *Ultra wideband systems: technologies and applications*. Newnes, 2006.
2. D. Dardari, A. Conti, U. Ferner, A. Giorgetti, and M. Z. Win, "Ranging with ultrawide bandwidth signals in multipath environments," *Proceedings of the IEEE*, vol. 97, no. 2, pp. 404–426, 2009.
3. E. Lagunas, M. Nájar, and M. Navarro, "Joint TOA and DOA estimation compliant with IEEE 802.15.4a standard," in *5th*

International Symposium on Wireless Pervasive Computing (ISWPC), vol. 97. IEEE, 2010, pp.157–162.

4. M. Nájar and M. Navarro, "Joint synchronization and demodulation for IR-UWB," in *IEEE International Conference on Ultra-Wideband (ICUWB)*, vol. 2, 2008, pp. 55-58.
5. M. Navarro and M. Najar, "TOA and DOA estimation for positioning and tracking in IR-UWB," in *IEEE International Conference on UltraWideband (ICUWB)*, 2007, pp. 574–579.
6. L. Osman, I. Sfar, and A. Gharsallah, "An overview of directionof-arrival estimation using a uniform linear antenna array with four elements," *American Journal of Applied Sciences*, pp. 1979–1984, 2012.
7. J. Vidal, M. Nájar, and R. Játiva, "High resolution time-of-arrival detection for wireless positioning systems," in *in Proc.* 56th *IEEE Vehicular Technology Conference (VTC)*, vol. 4, 2002, pp. 2283–2287.
8. V. Vu, A. J. Braga, B. Huyart, and X. Begaud, "Joint TOA/DOA measurements for spatio-temporal characteristics of 2.4 GHz indoor propagation channel," in *The European Conference on Wireless Technology*. IEEE, 2005, pp. 47–50.
9. V.V.Mani and R.Bose, "Smart antenna design for beamforming of UWB signals in gaussian noise," in *IEEE International ITG Workshop on Smart Antennas (WSA)*, 2008, pp. 311–316.
10. V.V.Mani and R. Bose, "Direction of arrival estimation and beamforming of multiple coherent UWB signals," in *IEEE International Conference on Communications (ICC)*, 2010, pp. 1–5.
11. G. Bing, X. Yi-tao, L. Jia, and L. Zhong-jun, "A robust autofocusing approach for estimating directions-of-arrival of wideband signals," *International Journal of Wireless and Microwave Technologies (IJWMT)*, vol. 2, no. 4, p. 28, 2012.
12. H. Keshavarz, "Weighted signal-subspace direction-finding of ultrawideband sources," in *International Conference on Wireless And Mobile Computing, Networking And Communications, (WiMob)*, vol. 1. IEEE, 2005, pp. 23–29.
13. D. Porcino and W. Hirt, "Ultra-wideband radio technology: potential and challenges ahead," *IEEE Communications Magazine*, vol. 41, no. 7, pp. 66–74, 2003.
14. K. Siwiak and D. McKeown, *Ultra-wideband radio technology*. John Wiley & sons, Inc.,, 2005.
15. M.Ghavami and Kohno.R, *Ultra wideband signals and systems in communication engineering*. John Wiley & Sons, Inc., 2004.
16. P. Vial, B. J. Wysocki, and T. A. Wysocki, "An ultra wide band simulator using MATLAB/simulink," *4th Workshop on the Internet, Telecommunications and Signal Processing*, p. 46, 2005.
17. C. M. Canadeo, "Ultra wide band multiple access performance using TH-PPM and DS-BPSK modulations," DTIC Document, Tech. Rep., 2003.
18. S. Yang and I. Darwazeh, "UWB propagation channel modeling," *Department of Electronic & Electrical Engineering, University College London*.
19. R. Zekavat and R. M. Buehrer, *Handbook of position location: Theory, practice and advances*. John Wiley & sons, Inc.,, 2011, vol. 27.
20. A. Rabbachin, J.-P. Montillet, P. Cheong, G. T. de Abreu, and I. Oppermann, "Non coherent energy collection approach for TOA estimation in UWB systems," in *Proceedings of the IST Mobile & Wireless Communications Summit*, 2005.
21. H. Jiang, Z.-J. Li, and D. Liu, "DOA estimation of ultra wideband signals using multiple constant beamwidth beamformers," in *International Conference on Wireless Communications & Signal Processing, (WCSP)*. IEEE, 2009, pp. 1–5.
22. P. Kabal and S. Valaee, "Selection of the focusing frequency in wideband array processing-MUSIC and ESPRIT," *Proc. Biennial Symp. Commun. (Kingston, Ont.)*, pp. 410–414, May 1992.
23. S. Valaee and P. Kabal, "The optimal focusing subspace for coherent signal subspace processing," *IEEE Transactions on Signal Processing*, vol. 44, no. 3, pp. 752–756, 1996.
24. I. Oppermann, M. Hämäläinen, and J. Iinatti, *UWB: theory and applications*. John Wiley & sons, Inc. 2005.